Superconductivity Induced by Phosphorus Doping and Its Coexistence with Ferromagnetism in $EuFe_2(As_{0.7}P_{0.3})_2$

Zhi Ren,[1] Qian Tao,[1] Shuai Jiang,[1] Chunmu Feng,[2] Cao Wang,[1] Jianhui Dai,[1] Guanghan Cao,[1,*] and Zhu'an Xu[1,†]

[1]*Department of Physics, Zhejiang University, Hangzhou 310027, China*

[2]*Test and Analysis Center, Zhejiang University, Hangzhou 310027, China*

(Received 19 January 2009; published 1 April 2009)

We have studied $EuFe_2(As_{0.7}P_{0.3})_2$ by the measurements of x-ray diffraction, electrical resistivity, thermopower, magnetic susceptibility, magnetoresistance, and specific heat. Partial substitution of As with P results in the shrinkage of lattice, which generates chemical pressure to the system. It is found that $EuFe_2(As_{0.7}P_{0.3})_2$ undergoes a superconducting transition at 26 K, followed by ferromagnetic ordering of Eu^{2+} moments at 20 K. This finding is the first observation of superconductivity stabilized by internal chemical pressure, and supplies a rare example showing the coexistence of superconductivity and ferromagnetism in the ferroarsenide family.

DOI: 10.1103/PhysRevLett.102.137002 PACS numbers: 74.70.Dd, 74.10.+v, 74.25.Ha, 74.62.Dh

Recently, high-temperature superconductivity has been discovered in a family of materials containing FeAs layers [1–4]. The superconductivity is induced by doping charge carriers into a parent compound, characterized by an antiferromagnetic spin-density-wave (SDW) transition associated with the FeAs layers [5,6]. Electron doping has been realized by the partial substitutions of F for O [1], vacancy for O [3], Th for Ln [4], and Co/Ni for Fe [7–10]. Examples of hole doping include the partial substitutions of Sr for Ln [11] and K for Ba/Sr/Eu [12–14]. All the chemical doping suppresses the long-range SDW order, eventually resulting in the emergence of superconductivity. Up to now, no superconductivity has been reported through doping at the As site. Apart from carrier doping, application of hydrostatic pressure is also capable of stabilizing superconductivity [15–17].

Among the parent compounds in the ferroarsenide family, $EuFe_2As_2$ exhibits peculiar behavior because the moments of Eu^{2+} ions order antiferromagnetically at relatively high temperature of 20 K [18–20]. Magnetoresistance measurements on $EuFe_2As_2$ crystals [21] suggest a strong coupling between the magnetism of Eu^{2+} ions and conduction electrons, which may affect or even destroy superconductivity. For example, though Ni doping in $BaFe_2As_2$ leads to superconductivity up to 21 K [10], ferromagnetism rather than superconductivity was found in $EuFe_2As_2$ by a systematic Ni doping [22]. Another relevant example is that the superconducting transition temperature of (Eu, K)Fe_2As_2 [14] is 32 K, substantially lower than those of (Ba, K)Fe_2As_2 ($T_c = 38$ K) [12] and (Sr, K)Fe_2As_2 ($T_c = 37$ K) [13]. Resistivity measurement under hydrostatic pressures [17] on $EuFe_2As_2$ crystals showed a resistivity drop at 29.5 K. However, no zero resistivity could be achieved, which was ascribed to the antiferromagnetic ordering of the Eu^{2+} moments [17].

While heterovalent substitution generally induces charge carriers, isovalent substitution may supply chemical pressure. The latter substitution is of particular interest in $EuFe_2As_2$ when As is partially replaced by P, as suggested theoretically in order to search for the magnetic quantum criticality without changing the number of Fe 3*d* electrons [23]. In this Letter, we demonstrate bulk superconductivity at 26 K in $EuFe_2(As_{0.7}P_{0.3})_2$. For the first time, superconductivity has been realized through doping at the As site in the ferroarsenide system. Strikingly, we observe coexistence of ferromagnetic ordering of Eu^{2+} moments with superconductivity below 20 K.

Polycrystalline samples of $EuFe_2(As_{0.7}P_{0.3})_2$ were synthesized by solid state reaction with EuAs, Fe_2As, and Fe_2P. EuAs was presynthesized by reacting Eu grains and As powders at 873 K for 10 h, then 1073 K for 10 h, and finally 1223 K for another 10 h. Fe_2As was prepared by reacting Fe powers and As powders at 873 K for 10 h then 1173 K for 0.5 h. Fe_2P was presynthesized by heating Fe powders and P powders very slowly to 873 K and holding for 10 h. Powders of EuAs, Fe_2As, and Fe_2P were weighed according to the stoichiometric ratio, ground and pressed into pellets in an argon-filled glovebox. The pellets were sealed in evacuated quartz tubes and annealed at 1273 K for 20 h then cooled slowly to room temperature. The phase purity of the resultant samples was investigated by powder x-ray diffraction (XRD), using a D/Max-rA diffractometer with Cu-K_α radiation and a graphite monochromator. The XRD data were collected in a step-scan mode for $10° \leq 2\theta \leq 120°$. The structural refinement was performed using RIETAN 2000 [24].

The electrical resistivity was measured on bar-shaped samples using a standard four-terminal method. The applied current density was ~ 0.5 A/cm^2. The measurements of magnetoresistance, specific heat, ac magnetic susceptibility, and thermopower were performed on a Quantum Design Physical Property Measurement System (PPMS-9). dc magnetic properties were measured on a Quantum Design Magnetic Property Measurement System (MPMS-5).

Figure 1 shows the XRD pattern of $EuFe_2(As_{0.7}P_{0.3})_2$ at room temperature, together with the profile of the Rietveld

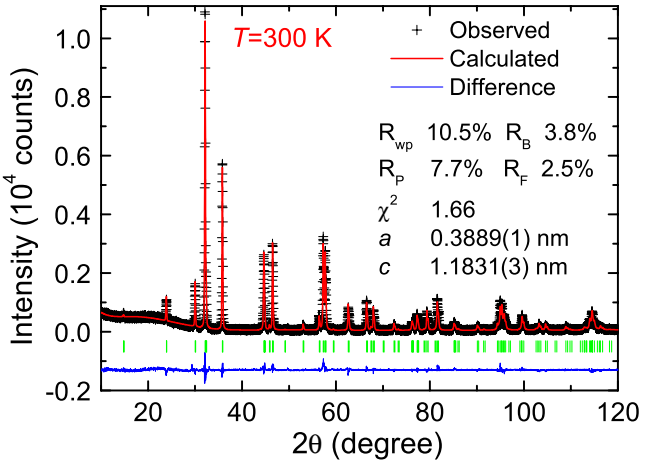

FIG. 1 (color online). X-ray powder diffraction pattern at room temperature and the Rietveld refinement profile for $EuFe_2(As_{0.7}P_{0.3})_2$.

refinement using the space group of $I4/mmm$. No additional diffraction peak is observed. The refined lattice parameters are $a = 3.889(1)$ Å and $c = 11.831(3)$ Å. Compared with those of the undoped $EuFe_2As_2$ [19], the a axis decreases by 0.35%, the c axis shortens by 1.8%, and the cell volume shrinks by 3.2% for $EuFe_2(As_{0.7}P_{0.3})_2$. These results suggest that the isovalent substitution of As with P indeed generates chemical pressure to the system. In addition, the As/P position z decreases from 0.3626(1) to 0.3620(1), indicating that the As/P atoms move toward the Fe planes. As a consequence, the Fe-(As/P)-Fe angle increases from 110.1(1)° to 111.5(1)°.

Figure 2(a) shows the temperature dependence of resistivity (ρ) and thermopower (S) for $EuFe_2(As_{0.7}P_{0.3})_2$ under zero field. The anomaly associated with the SDW transition in undoped $EuFe_2As_2$ [19] is completely suppressed. The resistivity decreases linearly with temperature down to ~90 K and shows upward deviation from the linearity at lower temperatures. The resistivity ratio of $R(300\ \mathrm{K})/R(30\ \mathrm{K})$ is 5.2, indicating high quality of the present sample. Below 29 K, the resistivity drops steeply, suggesting a superconducting transition. The midpoint of the transition is 26 K. On closer examination, shown in the inset of Fig. 2(a), however, a small resistivity peak is observed around 16 K, which coincides with the ferromagnetic ordering of Eu^{2+} moments (to be shown below). This observation is reminiscent of the reentrant superconducting behavior as observed, for example, in $RNi_2B_2C_2$ (R = Tm, Er, Ho)[25]. The thermopower shown in the right axis is negative in the whole temperature range, indicating that the dominant charge carriers are electronlike. $|S|$ decreases sharply below 26 K, corresponding to the superconducting transition. However, the $|S|$ value does not drop to zero until ~13 K, in relation with the ferromagnetic ordering of the Eu^{2+} moments.

In Fig. 2(b), we show the temperature dependence of field-cooled (FC) dc magnetic susceptibility for

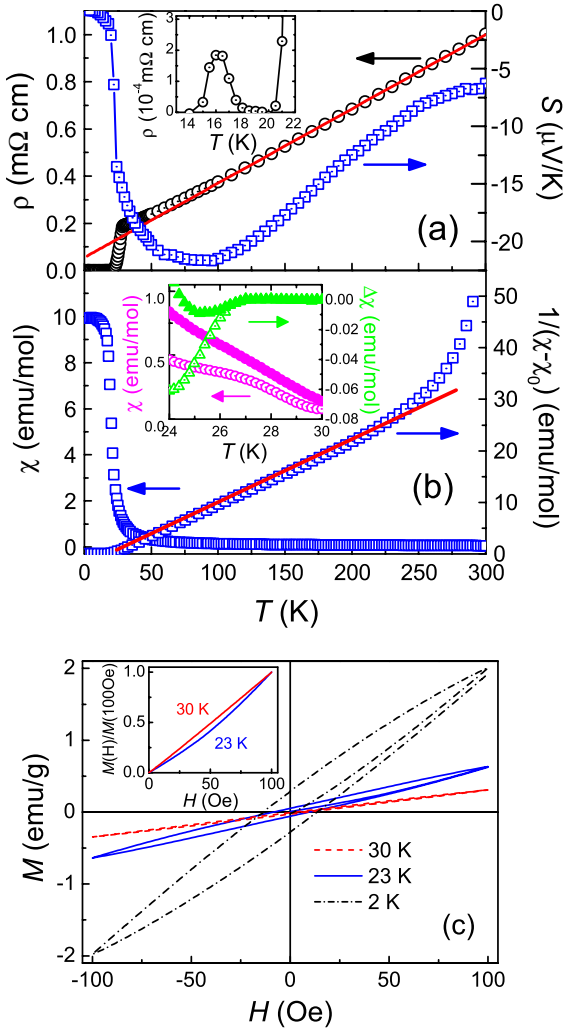

FIG. 2 (color online). Temperature dependence of resistivity together with thermopower (a), and magnetic susceptibility (b) for $EuFe_2(As_{0.7}P_{0.3})_2$. The inset of (a) shows an expanded plot of resistivity. The inset of (b) shows the ZFC (open symbols) and FC (solid symbols) susceptibilities (left axis) under $H_{dc} = 5$ Oe. Diamagnetic signals (right axis) are obtained after subtraction of the magnetic background. (c) Shows field dependence of magnetization (M) at various temperatures. The inset displays $M/M(100\ \mathrm{Oe})$ for 23 and 30 K.

$EuFe_2(As_{0.7}P_{0.3})_2$ under $H_{dc} = 1$ kOe. The obvious deviation of linearity in $(\chi - \chi_0)^{-1}$ above 230 K is probably due to the presence of trace amount of ferromagnetic Fe_2P impurity [26]. The χ data between 50 and 200 K can be well described by the modified Curie-Weiss law, $\chi = \chi_0 + C/(T - \theta)$, where χ_0 denotes the temperature-independent term, C the Curie-Weiss constant, and θ the paramagnetic Curie temperature. The fitting yields $\chi_0 = 0.044(1)$ emu/mol, $C = 8.1(1)$ emu · K/mol, and $\theta = 22(1)$ K. The very large value of χ_0 mainly comes from the ferromagnetic impurity. The effective moment is calculated to be $P_{\mathrm{eff}} = 8.0(1)\mu_B$ per formula unit (f.u.), close to the theoretical value of $7.94\mu_B$ for a free Eu^{2+} ion. Below 20 K, χ increases steeply with decreasing tempera-

ture and becomes gradually saturated. Field dependence of magnetization gives a saturated magnetic moment of $6.9(1)\mu_B$/f.u., as expected for fully paralleled Eu^{2+} moments with $S = 7/2$. Therefore, it is concluded that the moments of Eu^{2+} order ferromagnetically in $EuFe_2(As_{0.7}P_{0.3})_2$, in analogy with $EuFe_2P_2$ [27]. Because of the proximity of superconducting transition and ferromagnetic ordering, the superconducting diamagnetic signal is relatively weak. As shown in the inset of Fig. 2(b), a kink is observed around 26 K in the zero-field-cooled (ZFC) susceptibility measured under $H_{dc} = 5$ Oe while the anomaly in the FC data is less pronounced. After subtraction of the magnetic background, diamagnetic signals are seen in both the ZFC and FC data, confirming superconductivity in $EuFe_2(As_{0.7}P_{0.3})_2$. Figure 2(c) displays the isothermal magnetization. Superconductivity is inferred by the concave $M - H$ curve at 23 K, compared with the straight one at 30 K, shown in the inset.

The temperature dependence of resistivity under magnetic fields is shown in Fig. 3. With increasing magnetic fields, the resistive transition shifts towards lower temperature and becomes broadened, further affirming the superconducting transition. The $T_c(H)$, defined as a temperature where the resistivity falls to 50% of the normal-state value, is plotted as a function of magnetic field in the inset of Fig. 3. The $\mu_0 H_{c2}$-T diagram shows a slight upward curvature, which is probably due to the multiband effect [28]. The initial slope $\mu_0 \partial H_{c2}/\partial T$ near T_c is -1.18 T/K, giving an upper critical field of $\mu_0 H_{c2}(0) \sim 30$ T by linear extrapolation. It is also noted that the reentrant superconducting behavior is not obvious under magnetic field, in contrast with that in $RNi_2B_2C_2$ superconductors [25].

Figure 4 shows the result of specific-heat (C) measurements for the $EuFe_2(As_{0.7}P_{0.3})_2$ sample. Two anomalies below 30 K are identified. One is a λ-shape peak with the onset at 20 K, indicating a second-order transition. With increasing magnetic fields, the anomaly shifts to higher temperatures and becomes broadened, in accordance with a ferromagnetic nature of the transition. The other anomaly is much weaker but detectable at ~26 K (shown in the upper-left panel of Fig. 4), which coincides with the superconducting transition.

To analyze the $C(T)$ data further, it is assumed that the total specific heat consists of the electronic, phonon, and magnetic components. At high temperatures, the dominant contribution comes from the phonon component, which can be well described by the Debye model with only one adjustable parameter (i.e., Debye temperature Θ_D). The data fitting above 100 K gives $\Theta_D \approx 345$ K. Since $\Theta_D \sim 1/\sqrt{M}$ (M is the molecular weight), the Θ_D for $EuFe_2(As_{0.7}P_{0.3})_2$ is calculated to be 348 K, in good agreement with the fitted value, using the Θ_D data of 380 K for $EuFe_2P_2$ [27]. The upper bound of the electronic specific-heat coefficient is then estimated to be 10 mJ/mol $\cdot$ K^2, which is comparable with those of other iron-arsenide superconductors. The electronic specific-heat contribution is less than 2% of the total specific heat even at low temperatures, and thus is not taken into consideration in the following analysis.

By subtracting the lattice contribution, the specific anomaly due to the superconducting transition is more prominent. The jump in specific heat $\Delta C \approx 300$ mJ/mol $\cdot$ K at T_c is of the same order as that in $Ba_{0.55}K_{0.45}Fe_2As_2$ crystals [29]. Meanwhile, the magnetic entropy associated with the ferromagnetic transition is 16.5 J/mol $\cdot$ K, which amounts to 95% of $R\ln(2S + 1)$ with $S = 7/2$ for Eu^{2+} ions. The thermodynamic properties indicate that the superconducting transition and the ferromagnetic ordering are both of bulk nature.

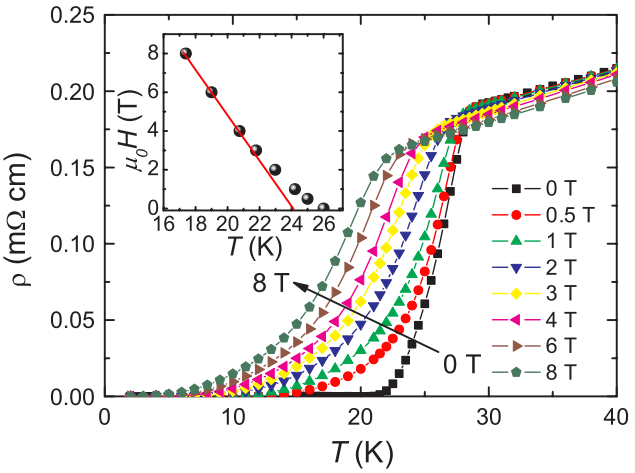

FIG. 3 (color online). Field dependence of resistive transition for $EuFe_2(As_{0.7}P_{0.3})_2$ sample. The inset shows the upper critical fields as a function of temperature.

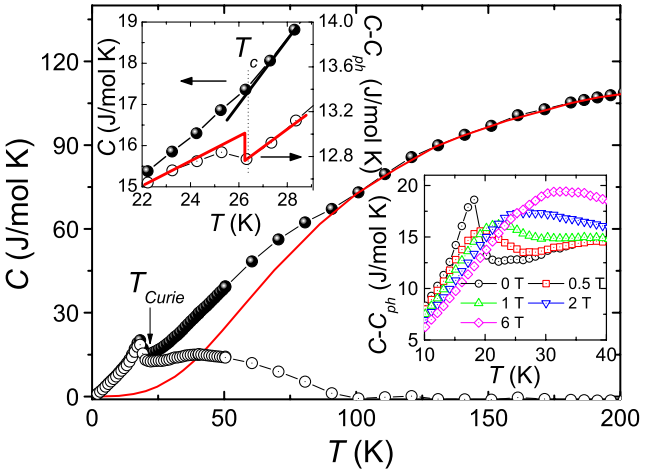

FIG. 4 (color online). Temperature dependence of specific heat before (solid symbols) and after (open symbols) deduction of lattice contribution for $EuFe_2(As_{0.7}P_{0.3})_2$. The solid curve represents the lattice contribution fitted by the Debye model. The upper-left panel shows the specific-heat anomaly around 26 K, which is ascribed to the superconducting transition. The lower-right panel shows the magnetic specific-heat anomaly around 20 K under magnetic fields.

A broad specific-heat hump below 90 K is evident after deduction of the lattice contribution, indicating existence of additional magnetic contribution. This anomaly is accompanied with the upward deviation from the linear temperature dependence in resistivity as shown in Fig. 2(a). Meanwhile, negative magnetoresistance was observed in the same temperature range, and reaches -6% at 30 K under $\mu_0 H = 8$ T (data not shown here). All these features are tentatively attributed to the interaction between the moments of Eu^{2+} ions and conduction electrons. Such interaction may be responsible for the observed ferromagnetic ordering of Eu^{2+} moments below 20 K [22].

The isovalent substitution of As with P does not change the number of Fe $3d$ electrons, but generates chemical pressure, as manifested by the shrinkage of lattice. This doping strategy contrasts with the heterovalent substitution of Eu with K [14,30] though the SDW transition is suppressed in both cases. According to a coherent-incoherent scenario [23], the low-energy physics of the FeAs-containing system is described by the interplay of the coherent excitations (associated with the itinerant carriers) and incoherent ones (modeled in terms of Fe localized magnetic moments). The internal chemical pressure generated via P doping results in the enhancement of coherent spectral weight, which weakens the SDW ordering and possibly induces a magnetic quantum critical point (QCP). In the structural point of view, the P doping results in closer distance between As/P and Fe planes. Accordingly, low-energy band width becomes larger (correspondingly the coherent spectral weight is enhanced), based on related band calculations [31]. Furthermore, magnetic fluctuations near the QCP may induce superconductivity, as has been well documented in the literature [32]. This explains the simultaneous suppression of SDW transition and emergence of superconductivity in $EuFe_2(As_{0.7}P_{0.3})_2$ assuming that a QCP occurs around a P content of $\sim 30\%$.

The superconducting properties of $EuFe_2(As_{0.7}P_{0.3})_2$ bear similarities with those of $EuFe_2As_2$ crystals under hydrostatic pressure [17]. As a matter of fact, the onset temperature of resistive drop is nearly the same in both cases, suggesting that the effect of internal chemical pressure is analogous to the application of external physical pressure. Thus it is expectable to find superconductivity in other iron-arsenide systems via the P-doping strategy.

In summary, we have found superconductivity at 26 K in $EuFe_2(As_{0.7}P_{0.3})_2$. Moreover, ferromagnetic ordering of Eu^{2+} moments coexists with the superconductivity below 20 K. The observation of sizable anomalies in thermodynamic properties, concomitant with the transitions, indicates that both are bulk phenomena. The interplay of superconductivity and ferromagnetism may bring about exotic properties and provide clues to the superconductivity mechanism, which renders $EuFe_2(As_{1-x}P_x)_2$ worthy of further exploration.

This work is supported by the NSF of China, National Basic Research Program of China (No. 2007CB925001), and the PCSIRT of the Ministry of Education of China (IRT0754).

*ghcao@zju.edu.cn
†zhuan@zju.edu.cn

[1] Y. Kamihara *et al.*, J. Am. Chem. Soc. **130**, 3296 (2008).
[2] X. H. Chen *et al.*, Nature (London) **453**, 761 (2008); G. F. Chen *et al.*, Phys. Rev. Lett. **100**, 247002 (2008).
[3] Z. A. Ren *et al.*, Europhys. Lett. **83**, 17 002 (2008); H. Kito, H. Eisaki, and A. Iyo, J. Phys. Soc. Jpn. **77**, 063707 (2008).
[4] C. Wang *et al.*, Europhys. Lett. **83**, 67 006 (2008).
[5] J. Dong *et al.*, Europhys. Lett. **83**, 27 006 (2008).
[6] C. de la Cruz *et al.*, Nature (London) **453**, 899 (2008).
[7] A. S. Sefat *et al.*, Phys. Rev. B **78**, 104505 (2008); C. Wang *et al.*, Phys. Rev. B **79**, 054521 (2009).
[8] A. S. Sefat *et al.*, Phys. Rev. Lett. **101**, 117004 (2008); A. Leithe-Jasper, W. Schnelle, C. Geibel, and H. Rosner, Phys. Rev. Lett. **101**, 207004 (2008).
[9] G. H. Cao *et al.*, arXiv:0807.4328.
[10] J. L. Li *et al.*, New J. Phys. **11**, 025008 (2009).
[11] H. H. Wen *et al.*, Europhys. Lett. **82**, 17 009 (2008).
[12] M. Rotter, M. Tegel, and D. Johrendt, Phys. Rev. Lett. **101**, 107006 (2008).
[13] K. Sasmal *et al.*, Phys. Rev. Lett. **101**, 107007 (2008); G. F. Chen *et al.*, Chin. Phys. Lett. **25**, 3403 (2008).
[14] H. S. Jeevan *et al.*, Phys. Rev. B **78**, 092406 (2008).
[15] M. S. Torikachvili, S. L. Budko, N. Ni, and P. C. Canfield, Phys. Rev. Lett. **101**, 057006 (2008); T. Park *et al.*, J. Phys. Condens. Matter **20**, 322204 (2008).
[16] P. L. Alireza *et al.*, J. Phys. Condens. Matter **21**, 012208 (2009).
[17] C. F. Miclea *et al.*, arXiv:0808.2026.
[18] R. Marchand and W. Jeitschko, J. Solid State Chem. **24**, 351 (1978).
[19] Z. Ren *et al.*, Phys. Rev. B **78**, 052501 (2008).
[20] H. S. Jeevan *et al.*, Phys. Rev. B **78**, 052502 (2008).
[21] S. Jiang *et al.*, New J. Phys. **11**, 025007 (2009).
[22] Z. Ren *et al.*, Phys. Rev. B (to be published).
[23] J. H. Dai *et al.*, Proc. Natl. Acad. Sci. U.S.A. 106, 4118 (2009).
[24] F. Izumi *et al.*, Mater. Sci. Forum **321–324**, 198 (2000).
[25] H. Eisaki *et al.*, Phys. Rev. B **50**, 647 (1994).
[26] T. M. McQueen *et al.*, Phys. Rev. B **78**, 024521 (2008).
[27] H. Raffius *et al.*, J. Phys. Chem. Solids **52**, 787 (1991).
[28] F. Hunte *et al.*, Nature (London) **453**, 903 (2008).
[29] N. Ni *et al.*, Phys. Rev. B **78**, 014507 (2008).
[30] Anupam *et al.*, arXiv:0812.1131.
[31] V. Vildosola *et al.*, Phys. Rev. B **78**, 064518 (2008).
[32] P. Gegenwart, Q. Si, and F. Steglich, Nature Phys. **4**, 186 (2008).